The Effect of Solidification Defect on the Dross Formation During Re-melting of Aluminum 5182 Alloy RSI

Q. Han[1], W.A. Simpson[1], J.L. Zeh[2], E.A. Kenik[1], P. Angelini, and V.K. Sikka[1]

[1]Oak Ridge National Laboratory, Oak Ridge, TN 37831-6083
[2]Logan Aluminum Inc., P.O. Box 3000, Russellville, KY 42276

Abstract

This article addresses the effect of solidification defects, such as cracking and porosity, on dross formation during the remelting of aluminum 5182 alloy RSI. Remelting experiments were carried out to measure the dross formation. Optical and electron scanning microscopy were employed to characterize the solidification defects. It was found that a huge amount of dross was formed during the remelting of certain types of RSI which contained severe internal cavities such as interdendritic porosity and hot tears. These cavities provided continuous channels that exposed the internal interdendritic surfaces to the atmosphere outside of the RSI. As a result, an oxide layer was formed on the surfaces of the interdendritic pores. Aluminum grains were entrained in the oxide shell, resulting in a large amount of dross formation during the re-melting of 5182 aluminum RSI.

Introduction

Bulk aluminum alloys intended for re-melting are often cast in the form of large shapes, weighing from 320 to 900 kg (700 to 2000 pounds), known as "sows." In the aluminum recycling industries, aluminum scrap is recycled and cast into sows. A sow cast from the aluminum scrap is termed as a remelt secondary ingot or RSI. As a solid form of molten aluminum alloys, RSI can be easily transported from the smelter to cast house where they are re-melted and cast into billets or ingots. The RSI is produced by pouring molten aluminum into open top molds. Since the RSI is intended for re-melting, little attention has been paid to their internal qualities except for the internal cavities that may collect water during the transport and storage of the RSI and may present a serious safety issue during the remelting of the RSI [1-4].

Recently the aluminum industry began to realize that dross formation is another important issue during mleting of the RSI. The formation of dross turns aluminum alloy into oxides, resulting in a tremendous waste of energy. The amount of dross formation varies from RSI to RSI. Initially, it was speculated that the dross observed during the remelting of RSI might result from inclusions that existed in the melt and were trapped in the RSI by the aluminum dendrites during solidification. In order to validate this, a couple of aluminum 5182 alloy RSI ingots that were thought to contain severe internal defects were examined using advanced Non-Destructive Evaluation (NDE) techniques, such as x-ray and ultrasound scanning [5]. The extent of the inclusions detected was much less than were expected. Melting experiments were then carried out to investigate dross formation [5-7]. The results were surprising. Some of the solid aluminum specimens taken from the center of those RSI ingots were not able to be melted at 850°C (1562°F), about 212°C higher than the liquidus temperature of aluminum 5182 alloys [6]. These experiments showed a huge dross formation during the re-melting of aluminum 5182 alloy RSI. The possible mechanisms of dross formation in the RSI were suggested [5-6] but were not confirmed. This article discusses the effect of the solidification defects on the dross formation in RSI. More evidence is provided to support the argument that the huge dross formation is related to the solidification defects such as hot tearing and interdendritic pores. These defects expose the internal surfaces of the interdendritic porosity to the ambient atmosphere during solidification and remelting of the RSI.

Experimental Methods and Results

The major solidification defects in the aluminum 5182 alloy RSI are cracking and porosity. In order to evaluate the effect of cracking on dross formation, commercial aluminum 5182 RSI, with and without visible cracks on their top surface, were chosen for remelting experiments. In order to evaluate the effect of porosity on dross formation, aluminum RSI of different magnesium compositions were chosen. The composition of each of the aluminum RSI is given in Table I. The weight of the RSI was about 2000 pounds. The largest dimensions of a RSI were 1.16m (45.5 in.) long, 1.16m (45.5 in.) wide, and 0.33m (13 in.) tall. The RSI were made from 5182 alloy scraps melted using induction melting furnace. After the melt was poured into an open metal mold, the top surface of the RSI was cooled using a water spray.

Table I The Chemical Composition (wt.%) of the Experimental RSI.

SRI No.	Al	Si	Fe	Cu	Mn	Mg	Cr	Zn	Ti
1	Bal.	0.62	0.53	0.07	0.51	1.11	0.01	0.02	0.03
2	Bal.	0.07	0.20	0.07	0.30	4.08	0.004	0.09	0.01
3	Bal.	0.26	0.21	0.06	0.31	4.79	0.01	0.01	0.02

Melting experiments

Specimens were made by slicing the RSI shown in Figure 1. The central slice was 3.81 cm (1.5 in.) thick. A specimen weighing approximately 0.6 kg was then cut from the central slice for the melting experiments. The location of the specimen cut from the central slice is illustrated in Figure 1. The specimen dimensions were about 3.17 cm (1.25 in.) long, 3.17 cm (1.25 in.) wide, and 15.24 cm (6 in.) tall. The specimens were melted in a boron nitride coated graphite crucible. A Muffle furnace (resistant heating) was used for the melting experiments. After the furnace had been heated to 850°C, the crucible with the specimen at room temperature was charged into the furnace. The volume of the crucible was much smaller than that of the chamber of the furnace so the temperature in the furnace did not change much during the charging of the cool specimen. The aluminum in the crucible reached 850°C in less than 20 minutes after the crucible was charged into the furnace. After the specimen had been held in the furnace for two hours, the liquid in the crucible was cast into an ingot and its weight was measured. The amount of dross left in the crucible was also collected and measured. The amounts of dross formation during the melting experiments are given in Table II.

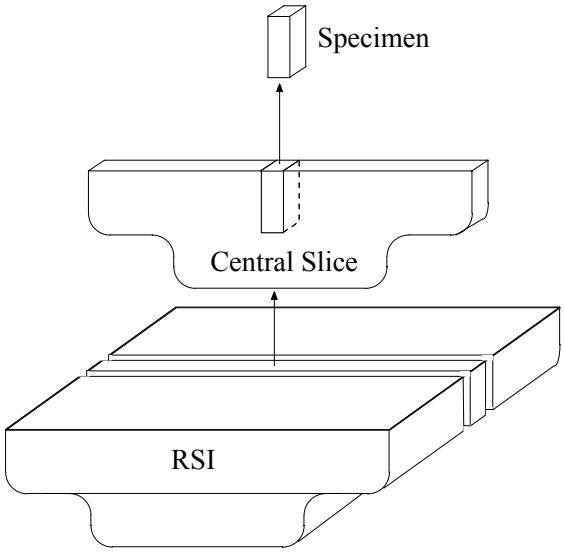

Figure 1: A schematic drawing illustrating the location of the specimen used for the remelting experiments.

Table II Results of the Remelting Experiments.

SRI No.	Dross Ratio (%)	Average Dross Ratio (%)	Remark
1	3.1	1.9	Spherical pores
	0.7		
2	22.1	22.9	Interdendritic pores
	25.6		
	9.3		
	37.0		
	20.7		
3	53.4	64.5	Cracking and interdendritic pores
	80.6		
	57.9		
	66.0		

Figure 2 shows a comparison of dross formation of RSI with and without cracks. The dross ratio shown in Figure 2 is defined as the weight of the dross over the weight of the specimen. For specimens taken from the RSI with crack on their top surface, the amounts of dross formation varied from 53 to 81%. In fact, these specimens didn't lose shape at 850°C. Dross formation was much less in the specimens taken from the RSI without cracks on its top surface. The amounts of dross formed during melting varied from 0.8 to 37%, a few times less than those RSI with cracks. For the specimens without cracks on the top surface of the RSI, dross formation occurred mainly on the top surface that had been water spray cooled during solidification. As pointed out in the reference 6, a highly porous layer, about 0.6 cm (0.25 in.) to 2.0 cm (0.75 in.) thick, existed on the top surface of the RSI due to water spray cooling. This layer turned into dross during the melting of the specimen.

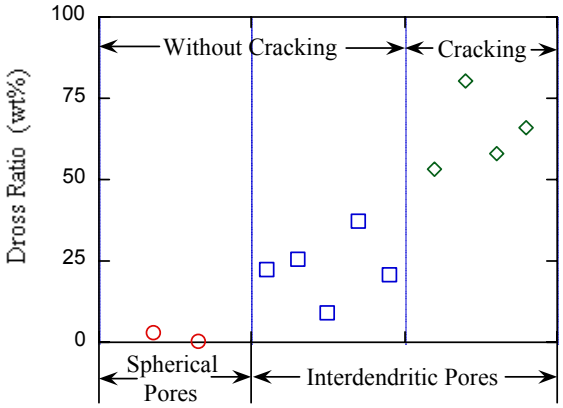

Figure 2: The amount of dross formed during the melting of specimens taken from the center of RSI.

Porosity morphology was also found to greatly affect the dross formation greatly. A comparison of dross formation in specimens containing interdendritic pores and spherical pores is also shown in Figure 2. Dross formation in the specimens containing interdendritic pores ranged from 9 to 37% for RSI with cracks and from 53 to 81% for RSI without cracks respectively. However, dross formation in the specimen containing spherical pores was only in the range between 0.7 to 3.1%, much less than the specimens containing interdendritic pores.

Microstructure characterization

The dross formed from the specimens taken from the RSI with cracks was characterized using optical microscopy and scanning electron microscopy (SEM). Figure 3 shows the microstructure of the dross. It contains aluminum dendrites and cavities identical to interdendritic pores that form during solidification due to hydrogen precipitation [8-10]. SEM images indicated that the aluminum dendrites were covered with a layer of oxides, more than 10 μm thick, see Figure 4. This explains the reason why the specimen didn't collapse at 850°C during the melting experiments. The oxides shown usually have high melting temperatures. At 850°C, the aluminum dendrites were melted but the oxides were still solid. As a result, the aluminum liquid was entrained in the oxide shell. It was the oxide-reinforced dendritic structure that prevented the specimen from collapsing at 850°C.

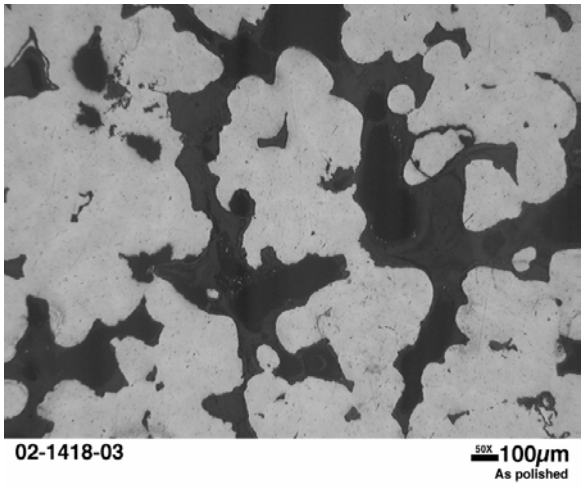

Figure 3: The microstructure on the as-polished surface of the dross formed during the remelting of a specimen taken from the center of a RSI. The white phase is the aluminum dendrites.

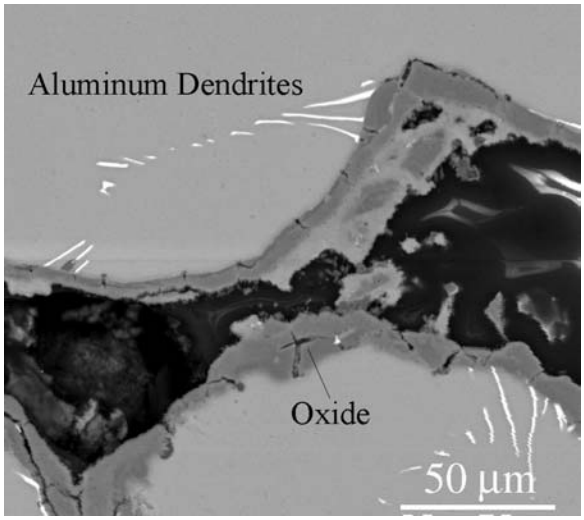

Figure 4: The SEM image of the dross, indicating that the aluminum dendrites are covered with a layer of oxides.

Figure 5 shows the as-cast microstructure of specimens taken from the center a RSI with surface cracks. The microstructure was mainly comprised of aluminum dendrites and interdendritic porosity. The porosity level was so high that the dendritic grains were almost separated by the interdendritic pores. An SEM image of the specimen is shown in Figure 6 and revealed an oxide layer on the surfaces of the interdendritic pores. In fact, the oxide layer shown in Figure 6 can be found everywhere on the specimen taken from the RSI with surface cracks. The oxide layer is fairly uniform in thickness. Energy dispersive X-ray spectroscopy (EDXS) analysis indicated that the oxide layer was comprised of two kinds of oxides. The outer bright regions shown in Figure 6 contain aluminum and oxygen and are likely alumina. The majority of the oxide is in the dark region of the oxide layer and contains aluminum, magnesium, and oxygen and is likely the mixed oxide $MgO.Al_2O_3$, known as spinel [11]. The oxides on the surfaces of pores in the center of the RSI, illustrated in Figure 6, are very similar to that shown in Figure 4 with respect to the oxide types and oxide layer thickness, except that small cracks exist on the oxide layer in the dross specimen. The small cracks shown in the oxide layer were formed during the heating stage of the melting experiments since the thermal expansion coefficient of the oxide is much smaller than that of the metal. Thus the major part of the oxide layer that entrained the liquid aluminum grains was formed in the solidification and the subsequent cooling stages of the RSI processing.

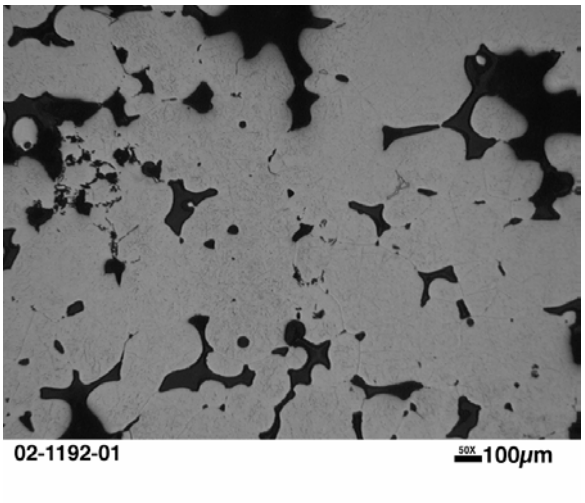

Figure 5: The as-cast microstructure of a specimen taken from the center of a RSI with surface cracks. On the surface of the as polished specimen, only aluminum dendrites and porosity can be seen.

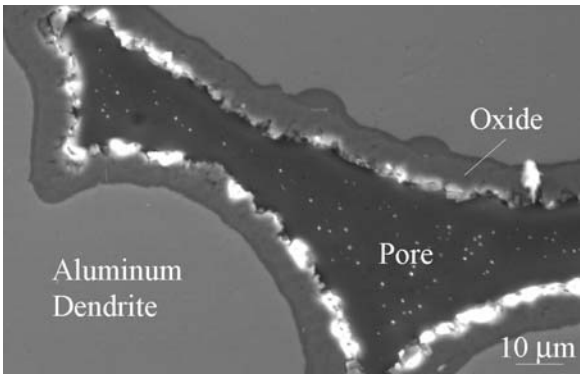

Figure 6: The SEM image of the as-cast microstructure. An oxide layer is formed on the surfaces of interdendritic pores. The bright regions on the interdendritic layer contain alumina. The majority of the oxide in the dark region of the layer is likely spinel.

Characterization of the cracks that are visible on the top surface of the RSI is shown in Figure 7. The SEM image was taken on the fracture surface of a cracked specimen. Clearly the fracture surface was dendritic. Arrays of dendrites were found everywhere on the fractured surface. This is a typical fracture morphology of hot tearing that occurs at temperatures higher than the non-equilibrium solidus temperature of the alloy [12-14]. Since the

fracture surface is totally comprised of dendrites, the liquid fraction at which fracture occurred should have been relatively high.

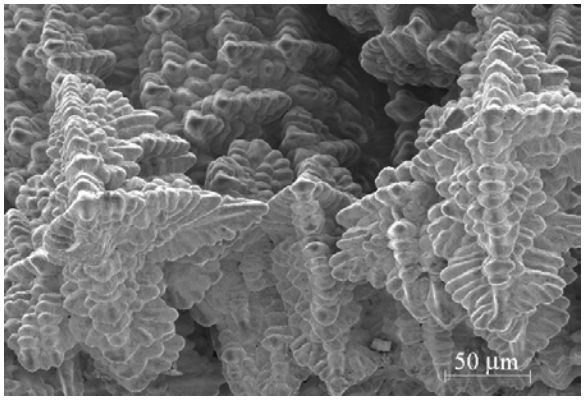

Figure 7: The SEM image of the fracture surface. Dendrites are clearly visible on the fracture surface, indicating the nature of the crack is hot tearing.

The microstructure in the specimen taken from the center of a RSI without surface cracking is shown in Figure 8 and is similar to those found with surface cracking. The porosity is also interdendritic. However, the volume fraction of the porosity seems lower than that shown in Figure 5, although the initial hydrogen concentrations in the RSI with and without surface cracks should be identical since they were produced under similar conditions. SEM analysis was also carried out to characterize the oxide layer on the pore surfaces in the center of the RSI. Some of the porosity surfaces had no oxide layer, shown in Figure 9. Other pores were found to be covered with a layer of oxides. In the porous layer near the top of the RSI, the pores were totally covered with oxides, as reported in reference 6. This accounted for the fact the most of the dross formed in these specimens was from the top porous layer due to water spray cooling during the solidification of the RSI.

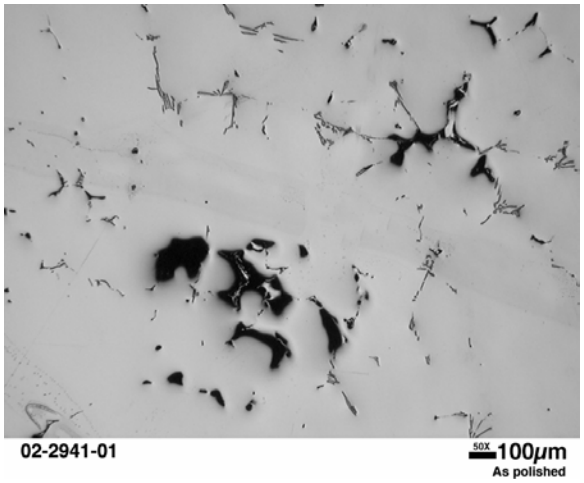

Figure 8: The as-cast microstructure of a specimen taken from the center of a RSI without surface cracks.

The as-cast microstructure of the RSI containing spherical pores is shown in Figure 10. These pores were more or less isolated. No oxides on the surface of the pore were found. This accounted for the low dross formation during the melting of the specimen containing spherical pores. The formation of the spherical pores was related to the low magnesium concentration of the alloy (see Table I). In the composition range given in Table I, the solidification interval of the alloy increases with increasing magnesium concentration [7]. At higher solidification intervals, dendritic structures are more fully developed. The morphology of the pores is determined by the dendritic structures.

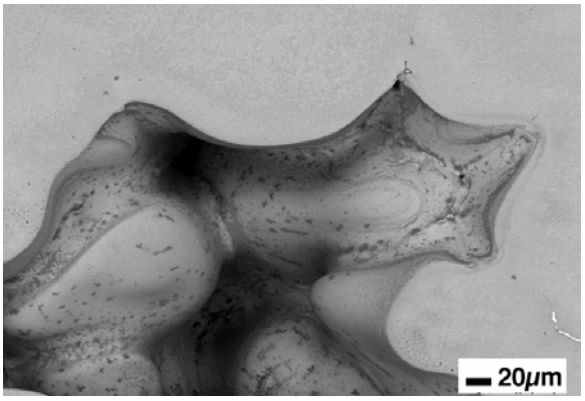

Figure 9: The SEM image of the as-cast microstructure. No oxide layer is formed on the surfaces of some interdendritic pores.

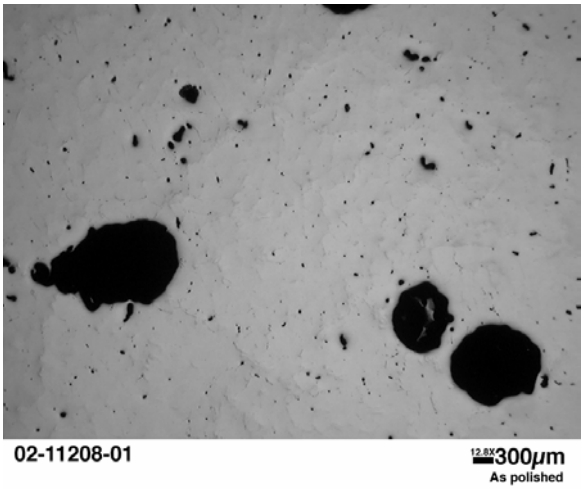

Figure 10: The as-cast microstructure of a specimen containing spherical pores. The pores are isolated.

Discussion

The results obtained in the remelting experiments indicated that the large amount of dross formation observed during the remelting of RSI was closely related to the internal cavities such as hot tearing and interdendritic porosity. Dross formation in RSI with hot tearing was much more than that in RSI without hot tearing. RSI containing interdendritic pores exhibited more dross formation than those containing spherical pores. Microstructural characterization of the as-cast specimens revealed a layer of

oxides on the surfaces of the interdendritic pores in the RSI having a high dross formation. This oxide layer was very much different in its morphology to the oxide films that were formed on top of the melt surfaces, brought into the melt by fluid flow during melting and pouring, and entrapped by the growing dendrites during solidification [11]. These results indicate that the oxide layer was formed *in-situ* on the surfaces of the interdendritic pores during the solidification and the subsequent cooling stages of the RSI processing. Furthermore, experiments using RSI containing spherical pores showed little dross formation. No oxide layer was found on specimens containing isolated spherical pores. All of our experimental evidence supports the hypothesis proposed in Reference 6 that the high dross formation is due to local oxidation on the surfaces of the interdendritic pores during the solidification and the subsequent cooling stages of the RSI processing. The internal cavities such as cracks and interdendritic porosity provide the pathways for oxygen/air to get into the center of the RSI.

Consider the solidification of a RSI. After molten aluminum alloy has been poured into a metal mold, a solid shell will be gradually formed on the mold surface. The RSI is also cooled at its top surface with water spray, which promotes the formation of a solid shell on the top of the RSI. Thus the central portion of the aluminum melt will be gradually enclosed in a solid shell. As solidification in the center of the RSI continues, the solidification shrinkage cannot be compensated, resulting in a reduced pressure within the solid shell. This reduced pressure tends to pull the top shell down, generating stresses in the top solid shell. If the stresses are higher than the strength of the material, hot tearing occurs. As soon as the top surface is fractured, air is pulled into the center of the RSI through the pathways of cracks and porosity. The air is then in direct contact with hot surfaces of the interdendritc pores at the center of the RSI, forming oxides in-situ on the porosity surfaces. The air contains oxygen that readily forms oxides on the pore surfaces at temperatures higher than the solidus temperature of the alloy. As a result, spinel forms on the surfaces of the interdendritic pores as air passes through these pores. Even if hot tearing is not formed, air is still likely to be pulled into the RSI by the reduced pressure at the center of the RSI since at high porosity levels the interdendritic pores are likely inter-connected and become permeable to air. In this case, the amount of air being pulled into the center of a RSI will be less than the case when the top surface was fractured, resulting in less dross formation than that in the fractured RSI. In cases where the pores are spherical and isolated, the solid shell will be not permeable to air. No air can be pulled into the solidifying RSI, and, therefore, less dross will be formed during the remelting of the RSI. Our experimental results support all of the above arguments.

Conclusion

The amount of dross formation during the remelting of RSI is closely related to the cavities such as cracks and porosity in the RSI. RSI with surface cracks exhibit higher dross formation than those without surface cracks. Dross formation in RSI containing interdendritic pores is higher than those containing spherical and isolated pores.

An oxide layer is found on the surfaces of the interdendritic pores in RSI having a large dross formation. This oxide layer is formed *in-situ* on the pore surfaces during the solidification and the subsequent cooling stages of the RSI processing. Hot tears and interdendritic pores provide pathways for air to be sucked into the center of the RSI. During remelting, much of the aluminum is entrained in the oxide layer. As a result, the entrained aluminum is being lost as dross.

Acknowledgment

This research was supported by the United States Department of Energy, Assistant Secretary for Energy Efficiency and Renewable Energy, Industrial Technologies Program, Industrial Materials for the Future (IMF) Program, Aluminum Industry of the Future, Materials Processing Laboratory Users (MPLUS) Facilities, under contract No. DE-AC05-00OR22725 with UT-Battelle, LLC. The authors would like to thank Logan Aluminum, Inc. for providing the ingot slices, J.R. Mayotte for optical metallography, E.C. Hatfield for the melting experiments, K.S. Reeves for part of the SEM work, T.J. Huxford and S. Babu for reviewing the article.

References

1. G.N. Chaffin, and J.E. Jacoby, "Guidlelines for Aluminum Sow Casting and Charging," (The Aluminum Association, p. 12).
2. S.G. Epstein, "Update on Molten Aluminum Incident Reporting," Light Metals 1997, ed. R. Huglen (Warrendale, PA: TMS 1997), 887-897.
3. A. Giron, and J.E. Jacoby, "Design of Molds to Minimize Internal Shrinkage Cavities in Sows," Light Metals 1993, ed. S.K. Das (Warrendale, PA: TMS, 1993), 855-861.
4. R.D. Peterson, R.D. White, and R. Downie, "Development and Verification of DELPEC Sow Mold," Light Metals 1992, ed. E.R. Cutshal (Warrendale, PA: TMS 1992), 999-1005.
5. W.A. Simpson, Q. Han, and J.L. Zeh, "Detection of Fabrication Defects in Aluminum Sows," (Report on MPLUS Project MC-01-012, Oak Ridge National Laboratory, May, 2002).
6. Q. Han, W.A. Simpson, J.L. Zeh, E.D. Hatfield, and V.K. Sikka, "Dross Formation during Re-melting of Aluminum 5182 Remelt Secondary Ingot (RSI)", Submitted to Metall. Trans.
7. Q. Han and J.L. Zeh, "Reducing Dross Formation during Remelting of 5182 Aluminum RSI," (Report on MPLUS Project MC-02-042, Oak Ridge National Laboratory, October, 2002).
8. T.S. Piwonka, and M.C. Flemings, "Pore Formation in Solidification," Trans. TMS-AIME, 236 (1966), 1157-1165.
9. D.R. Poirier, K. Yeum, and A.L. Maples, "A Thermodynamical Prediction for Microporosity Formation in Aluminum-Rich Al-Cu Alloys," Metall. Trans., 18A (1987), 1979-87.
10. Q. Han, and S. Viswanathan, "Hydrogen Evolution during Directional Solidification and Its Effect on Porosity Formation in Aluminum Alloys," Metall. Mater. Trans., 33A (2002), 2067-2072.
11. J. Campbell, Castings, (Butterworth-Heinemann, Oxford, United Kingdom, 1991), 15-23.
12. W.S. Pellini, "Strain Theory of Hot Tearing," Foundry, 80 (1952), 124-133.
13. M.C. Flemings, Solidification Processing, (McGraw-Hill, New York, 1974), 254.
14. Q. Han, S. Viswanathan, W. Spinhowell, and S. Das, "The Nature of Surface Cracking of the 3004 Aluminum DC Castings," Metall. Mater. Trans, 32A (2001), 2908-2910.